Available online at www.sciencedirect.com

ScienceDirect

IFAC Papers Online CONFERENCE PAPER ARCHIVE

IFAC-PapersOnLine 49-20 (2016) 096–101

Entropy-based estimation of bubble size distributions in froth flotation using B-spline functions ⋆

Jie Han, Chunhua Yang, Xiaojun Zhou, Weihua Gui

School of Information Science and Engineering, Central South University, Hunan 410083, China (e-mail: michael.x.zhou@csu.edu.cn).

Abstract: Bubble size distribution is an important feature in froth flotation processes and the B-spline estimation is a common way to approximate the bubble size distribution by using the least square algorithm. However, it is difficult to determine the number of basis functions of B-spline. In this study, the analysis based on the unbiased cross entropy is proposed to evaluate the estimated models. Experimental results have shown the feasibility and effectiveness of the proposed method.

Keywords: Froth flotation process, bubble size, probability density function, B-spline

1. INTRODUCTION

Froth flotation is a separation process aimed to extract valuable minerals from raw ore. As a multivariate process, froth flotation is influenced by multiple factors such as impeller speed, reagent addition and inlet air flow (Yang et al. [2009a]). Since the nature of underlying microscopic phenomena is chaotic and complicated, the modelling and control of flotation processes are difficult (Bao et al. [2008]). Experiences have shown that the efficiency of flotation process is highly correlated to the froth characteristics. In Moolman et al. [1996], the control of flotation processes is heavily dependent on the experience of human operators by observing the visual appearance of the surface froth, which varies with each individual and lacks objective criterion. However, with the advancement in digital image processing techniques, quantification of froth properties becomes particularly convenient.

As one of the dominant visual features, bubble size can provide important information about flotation process status (Feng. [2000]). For bauxite flotation, froth bubble size is not only related to technical indices such as concentrate grade and tailings grade, but also connected with technological parameters like pulp acidity and pulp density. In order to get generic relationships for the performance of flotation froths, Wang et al. [2009] proposed an empirical formula about bubble size distributions. It is worth noticing that the probability density function (PDF) of surface bubble size is found to be non-Gaussian, and Yang et al. [2009b] used nonparametric estimation technique to approximate this distribution. Based on the theory of stochastic distribution control, the output PDFs can be tracked to a target distribution shape by using control approaches (Guo et al. [2008]). Considering the relationship of bubble size distribution and the process of froth flotation, Zhu et al. [2014] proposed a novel reagent dosage predictive control method which was based on the PDF of bubble size.

Since the estimation of bubble size distribution is a prerequisite step of tracking a target distribution shape, a method using B-spline function and entropy to approximate the PDF of bubble size is proposed in this paper. This method includes three steps. First, the PDF of bubble size distribution is described by using kernel density estimators. Second, we use a linear combination of B-splines to approximate the kernel density estimation by least-squares method. Final step, the best model of linear combination is determined by entropy analysis. The proposed method can describe the bubble size distribution effectively by the weights of B-spline estimation, and it can be applied to the further control of flotation process.

The remainder of the paper is organized as follows. The mechanism of the gold-antimony flotation process and the approach of characterizing the bubble size are described in the section 2. Section 3 presents the B-spline estimator based on entropy and experimental results is discussed in Section4. Section 5 provides the conclusion of this paper.

2. PROCESS DESCRIPTION

2.1 Gold-antimony flotation process

The process of froth flotation makes use of the physicochemical properties of mineral grains to concentrate valuable materials. After grinding the raw ore to a fine size and mixing them with water, frothing reagents and collecting reagents, the pulp is fed in the flotation cells. The sparger at the bottom of the container can continuously inject air into the pulp to form a large number of bubbles (see Fig. 1). Chemical reagents can adjust the surface

⋆ This work was supported by the National Natural Science Foundation of China (Grant No. 61490702 and No. 61503416), the Innovation-driven Plan in Central South University (Grant No. 2015cx007) and the Foundation for Innovative Research Groups of the National Natural Science Foundation of China (Grant No. 61321003).

10.1016/j.ifacol.2016.10.103

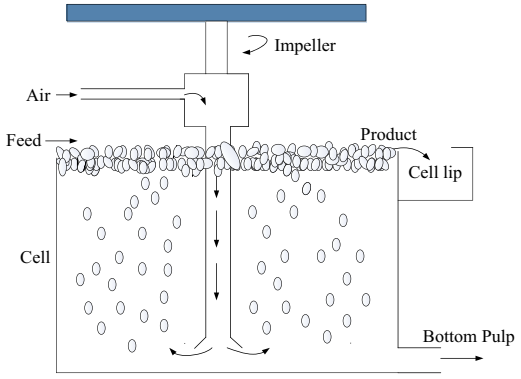

Fig. 1. The process of froth flotation

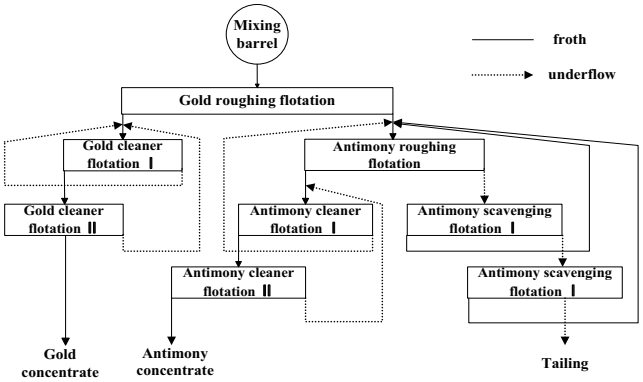

Fig. 2. Process flow of gold-antimony flotation

hydrophobicity of the fine particles. In general, the valuable material particles are hydrophobic and adhered to the bubble surface. Due to the flotage effect, air bubbles float to the top and can be used to collect concentrate product. The hydrophilic particles such as tailings settle to the bottom and are recycled for further treatment.

In this paper, the gold-antimony flotation is mainly studied and Fig. 2 shows its process flow (Wu et al. [2015]). The mineral particles containing gold are first selected by the gold roughing flotation and gold cleaner flotation I, II, the mineral particles containing antimony are then collected by the antimony roughing flotation and antimony cleaner flotation I, II. Scavenging flotation process is used to improve the recovery rate of minerals.

2.2 Bubble size feature extraction

Image measurement set-up for the flotation process always consists of a RGB camera and a lamp above the surface of the froth layer. As discovered, froth images collected from industry field show that each bubble has only one total reflectance point, and this property enables bubble segmentation to be much easier.

Although there are many methods about froth image segmentation, including valley-edge detection and tracing technique (Wang et al. [2003]), white spots detection (Wang et al. [2005]), watershed transformation (Bartolacci et al. [2001]) and wavelet approach (Liu et al. [2005]), they all have poor effect when dealing with the froth image

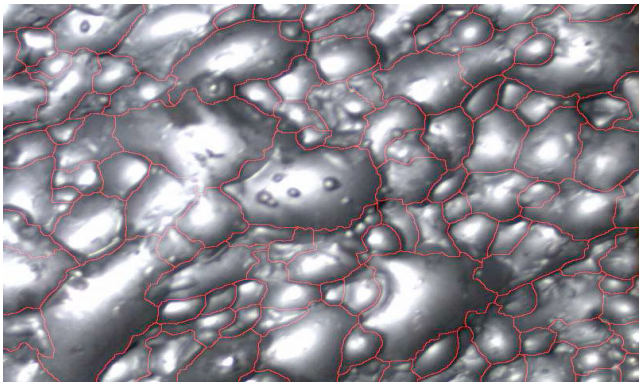

Fig. 3. The segmentation of froth image

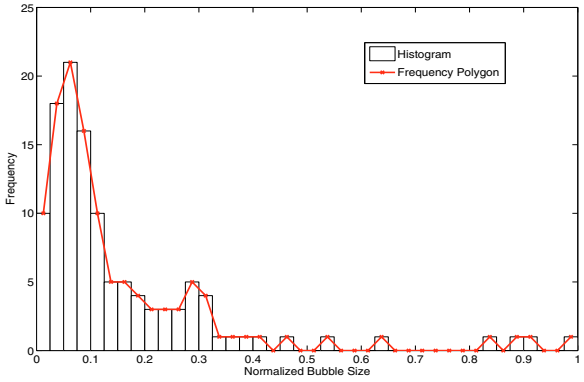

Fig. 4. The histogram and frequency polygon of bubble size distribution

with both large and tiny bubbles. In this paper, a two-pass watershed algorithm explored by Gordon Forbes (Forbes, G. [2007]) is adopted to segment image. Before using this algorithm, gray-scale dilations-based morphological reconstruction is applied to denoising. Fig. 3 shows the segmentation result of antimony roughing flotation image and Fig. 4 is the relevant histogram and frequency polygon of bubble size distribution.

3. B-SPLINE ESTIMATION BASED ON ENTROPY

3.1 B-spline estimation

There are many ways to estimate the irregular distribution of some random variables, especially histogram, frequency polygon, shift average histogram, kernel methods and B-spline expansion models (Zhang et al. [2006]). Since the control of froth flotation process can be considered as the control of the bubble size distribution and B-spline estimation can identify the PDF accurately with several wights, the control of froth flotation can be transformed to the control of weights in B-spline estimation. Then, the B-spline estimation is chosen to approximate bubble size PDF.

A linear combination of B-spline functions can be used to approximate the PDF of a continuous random variable from a given data. The equation of B-spline estimation $f(x,\alpha)$ of order k is given by

$$f(x,\alpha)=\sum_{i=1}^{n}\alpha_i B_{i,k}(x), t_{\min}\le x\le t_{\max} \qquad (1)$$

where x represents the random variable, α_i is the weights and n is the number of B-spline basis functions. $B_{i,k}(x)$ means the B-spline basis function of order k defined on a knot vector $\boldsymbol{T}$. The knot vector $\boldsymbol{T}$ consists of non-decreasing real-valued knots. The B-spline basis function can be recursively defined as

$$B_{i,k}(x) = \frac{(x-t_i)}{t_{i+k-1}-t_i}B_{i,k-1}(x) + \frac{(t_{i+k}-x)}{t_{i+k}-t_{i+1}}B_{i+1,k-1}(x) \tag{2}$$

where

$$B_{i,0} = \begin{cases} 1, & \text{if } t_i \le x \le t_{i+1} \\ 0, & \text{otherwise} \end{cases} \tag{3}$$

Since there may exist $0/0$, the definition $0/0 = 0$ is defined. In this paper, the second order B-spline function is used to approximate the PDF of bubble size, which is shown as follows:

$$B_{i,2} = \begin{cases} \dfrac{(x-t_i)^2}{(t_{i+2}-t_i)(t_{i+1}-t_i)} & \text{if } t_i \le x \le t_{i+1} \\ \dfrac{x-t_i}{t_{i+2}-t_i}\cdot\dfrac{t_{i+2}-x}{t_{i+2}-t_{i+1}} + & \\ +\dfrac{t_{i+3}-x}{t_{i+3}-t_{i+1}}\cdot\dfrac{x-t_{i+1}}{t_{i+2}-t_{i+1}} & \text{if } t_{i+1} \le x \le t_{i+2} \\ \dfrac{(t_{i+3}-x)^2}{(t_{i+3}-t_{i+1})(t_{i+3}-t_{i+2})} & \text{if } t_{i+2} \le x \le t_{i+3} \\ 0 & \text{otherwise} \end{cases} \tag{4}$$

The distribution range of $\boldsymbol{T}$ is $[a,b]$. Divide the range $[a,b]$ into $n-2$ equal intervals which have the following relationship:

$$a = t_0 < t_1 < t_2 < \cdots < t_{n-2} \tag{5}$$

For convenience, four extended nodes $t_{-2}, t_{-1}, t_{n-1}, t_n$ are added. Usually we take $t_{-2} = t_{-1} = t_0, t_{n-2} = t_{n-1} = t_n$.

The reasons why we use second order B-spline are about two aspects. On the one hand, as shown in equation (4), the second order B-spline function is a piecewise-quadratic function, and if the order increase, the form of B-spline function will be more complex which may cause high-computational cost. On the other hand, the second order B-spline already has the ability to fit all kinds of PDF.

3.2 Least squares approximation

The main idea of least squares approximation in this paper is to minimize the fitting error S between the given PDF $g(x)$ and the B-spline function $f(x,\alpha)$. The relationship of these two functions can be transformed to linear matrix equations:

$$\begin{bmatrix} B_{1,k}(x_1) & B_{2,k}(x_1) & \cdots & B_{n,k}(x_1) \\ B_{1,k}(x_2) & B_{2,k}(x_2) & \cdots & B_{n,k}(x_2) \\ \vdots & \vdots & \ddots & \vdots \\ B_{1,k}(x_m) & B_{2,k}(x_m) & \cdots & B_{n,k}(x_m) \end{bmatrix} \begin{bmatrix} \alpha_1 \\ \alpha_2 \\ \vdots \\ \alpha_n \end{bmatrix} = \begin{bmatrix} g_1 \\ g_2 \\ \vdots \\ g_m \end{bmatrix} \tag{6}$$

where m means the number of variables. These linear equations can be rewritten as $\boldsymbol{B}\cdot\boldsymbol{\alpha} = \boldsymbol{g}$ and the least square problem is defined as

$$Minimize\ S(\boldsymbol{\alpha}) = \|\boldsymbol{g} - \boldsymbol{B}\cdot\boldsymbol{\alpha}\|_2^2 = \Sigma(g(x) - f(x,\alpha))^2 \tag{7}$$

According to the theory of least square method, the weights can be calculated by

$$\boldsymbol{\alpha} = (\boldsymbol{B}^T\boldsymbol{B})^{-1}\boldsymbol{B}^T\boldsymbol{g} \tag{8}$$

Proof:

The squared residuals S between the $g(x)$ and $f(x,\alpha)$ can be rewritten as

$$\begin{aligned} S(\boldsymbol{\alpha}) &= \|\boldsymbol{g} - \boldsymbol{B}\boldsymbol{\alpha}\|_2^2 \\ &= (\boldsymbol{g} - \boldsymbol{B}\boldsymbol{\alpha})^T(\boldsymbol{g} - \boldsymbol{B}\boldsymbol{\alpha}) \\ &= \boldsymbol{g}^T\boldsymbol{g} - \boldsymbol{g}^T\boldsymbol{B}\boldsymbol{\alpha} - \boldsymbol{\alpha}^T\boldsymbol{B}^T\boldsymbol{g} + \boldsymbol{\alpha}^T\boldsymbol{B}^T\boldsymbol{B}\boldsymbol{\alpha} \end{aligned} \tag{9}$$

When S reaches the minimum value, the model function can fit the original data best. The minimum of $S(\boldsymbol{\alpha})$ is obtained by setting the derivatives of $S(\boldsymbol{\alpha})$ equal to zero. Note that the function $S(\boldsymbol{\alpha})$ has scalar values, whereas $\boldsymbol{\alpha}$ is a column vector with n components. So we have n first order derivatives and we will follow the convention to arrange them in a column vector. The second and third terms of the equation (9) are equal and may be replaced by $-2\boldsymbol{\alpha}^T\boldsymbol{B}^T\boldsymbol{g}$. The vector of derivatives equals $-2\boldsymbol{B}^T\boldsymbol{g}$. The last term of equation (9) is a quadratic form in the elements of $\boldsymbol{\alpha}$. The vector of first order derivatives of this term can be rewritten as $2\boldsymbol{B}^T\boldsymbol{B}\boldsymbol{\alpha}$. So, we can obtain

$$\frac{\partial S}{\partial \boldsymbol{\alpha}} = -2\boldsymbol{B}^T\boldsymbol{g} + 2\boldsymbol{B}^T\boldsymbol{B}\boldsymbol{\alpha} \tag{10}$$

By setting these derivatives equal to zero, the equation can be transformed to

$$\boldsymbol{B}^T\boldsymbol{B}\boldsymbol{\alpha} = \boldsymbol{B}^T\boldsymbol{g} \tag{11}$$

Solving this for $\boldsymbol{\alpha}$, we obtain

$$\boldsymbol{\alpha} = (\boldsymbol{B}^T\boldsymbol{B})^{-1}\boldsymbol{B}^T\boldsymbol{g} \tag{12}$$

3.3 Evaluation mechanism based on entropy

The number of B-spline basis functions (n) is an important parameter in estimation process. With different n, we can define different estimates of the PDF. In information theory, the cross entropy is a measure of the uncertainty associated with a random variable, and cross-entropy minimization is frequently used in probability estimation. When the cross-entropy reaches the minimum, the uncertainty of estimation will be minimized and this estimation can be considered as the best model. For the purpose of determining the best model of B-spline, the following entropy is applied to evaluate the fitting results (Zong. [1998]):

$$J(g,f) = -\int g(x)\log f(x)\mathrm{d}x \tag{13}$$

When $J(g,f)$ attain a minimum value, fitting function $f(x)$ is equal to original function $g(x)$. Considering the biased error of least square method, the asymptotically unbiased estimate of $H(g,f)$ is

$$E = \frac{3n_f}{2n_s} - \int g(x)\log f(x,\alpha)\mathrm{d}x \tag{14}$$

where n_s is the number of sample points, n_f is the number of free parameters in the model and equal to $n-1$ in this paper. In order to chose the best estimation of PDF, E must be minimized.

Proof:

Based on the information theory, suppose the PDF of a continuous random variable x is $g(x,\theta)$ where θ is

parameter vector, and let $f(x)$ be a candidate model, the entropy of x can be used to evaluate the model g:

$$J(g,f) = -\int g(x)\log f(x)\mathrm{d}x \tag{15}$$

Moreover

$$\begin{aligned} J(g,f) &= -\int g(x)\log f(x)\mathrm{d}x \\ &= -\int g(x)\log g(x)\mathrm{d}x + \int g(x)\log\frac{g(x)}{f(x)}\mathrm{d}x \\ &= J(g,g) + I(g,f) \end{aligned} \tag{16}$$

where $J(g,g) = -\int g(x)\log g(x)\mathrm{d}x$ is the entropy of x, $I(g,f)$ is the Kullback information which has the following properties:

(1) $I \geq 0$,

(2) $I = 0$ if and only if $g = f$.

So, we can obtain $J(g,f) = J(g,g) + I(g,f) \geq J(g,g)$. Thus, the entropy $J(g,f)$ attains minimum when estimated model equal to the true model.

The model $g(x)$ contains unknown parameter vector $\theta = (\theta_1, \cdots, \theta_{n_f})$. In order to estimate this parameter vector, a sample x is taken from the population. Here, suppose the least square estimate of θ is $\hat{\theta}$, and the least square estimate of entropy $J(g,g) = J(x,\theta)$ is $J(x,\hat{\theta})$. However, because the variance of least square estimator are biased, $J(x,\hat{\theta})$ is also a biased estimator of $J(x,\theta)$. In order to find the unbiased estimator, the following analysis is employed.

Expand $g(x,\hat{\theta})$ around the true value θ^0

$$g(x,\hat{\theta}) \approx g^0(x,\theta^0) + \frac{\partial g^0(x,\theta^0)}{\partial\theta_i}\Delta\theta_i \tag{17}$$

where

$$\frac{\partial g^0(x,\theta^0)}{\partial\theta_i}\Delta\theta_i = \sum_{i=1}^{k}\frac{\partial g^0(x,\theta^0)}{\partial\theta_i}\Delta\theta_i \tag{18}$$

Similarly,

$$\log g(x,\hat{\theta}) \approx \log g^0(x,\theta^0) + \frac{\partial\log g^0(x,\theta^0)}{\partial\theta_i}\Delta\theta_i \tag{19}$$

Let g^0 represents $g^0(x,\theta^0)$, so

$$\begin{aligned} J(x,\hat{\theta}) &= -\int g(x,\hat{\theta})\log g(x,\hat{\theta})\mathrm{d}x \\ &= -\int\{g^0 + \frac{\partial g^0}{\partial\theta_i}\Delta\theta_i\}\cdot \\ &\quad\cdot\{\log g^0 + \frac{\partial\log g^0}{\partial\theta_i}\Delta\theta_i\}\mathrm{d}x \\ &= -\int g^0\log g^0\mathrm{d}x \\ &\quad -[\int\{g^0\frac{\partial\log g^0}{\partial\theta_i} + \frac{\partial g^0}{\partial\theta_i}\log g^0\}\mathrm{d}x]\Delta\theta_i \\ &\quad -(\int\frac{\partial g^0}{\partial\theta_i}\frac{\partial\log g^0}{\partial\theta_i}\mathrm{d}x)\Delta\theta_i\Delta\theta_j \\ &= J(x,\theta^0) \\ &\quad -[\int\{g^0\frac{\partial\log g^0}{\partial\theta_i} + \frac{\partial g^0}{\partial\theta_i}\log g^0\}\mathrm{d}x]\Delta\theta_i \\ &\quad -(\int g^0\frac{\partial\log g^0}{\partial\theta_i}\frac{\partial\log g^0}{\partial\theta_j}\mathrm{d}x)\Delta\theta_i\Delta\theta_j \\ &= J(x,\theta^0) \\ &\quad -[\int\{g^0\frac{\partial\log g^0}{\partial\theta_i} + \frac{\partial g^0}{\partial\theta_i}\log g^0\}\mathrm{d}x]\Delta\theta_i \\ &\quad -\Delta\theta_i a_{ij}\Delta\theta_j \end{aligned} \tag{20}$$

where

$$a_{ij} = E_x\{\frac{\partial\log g^0}{\partial\theta_i}\frac{\partial\log g^0}{\partial\theta_j}\} \tag{21}$$

is a Fisherian information matrix. In the equation (20), the first term is the entropy measured by the true model, the second term is asymptotically a normal random variable with zero mean and the third term with mean n_f/n_s(Mood et al. [1974]), then

$$E_{\hat{\theta}}J(x,\hat{\theta}) + n_f/n_s = J(x,\theta^0) \tag{22}$$

where k is the number of free parameters in a model and n_s is the sample size. So

$$J(x,\theta^0) = J(x,\hat{\theta}) + n_f/n_s \tag{23}$$

Similar to the above arguments, the Kullback information $I(g,f)$ is given by

$$\hat{I}(g,f) = I(g,f) + \frac{n_f}{2n_s} \tag{24}$$

Finally, the asymptotically unbiased estimator of entropy $J(g,f)$ is

$$\hat{J}(g,f) = J(g,f) + \frac{3n_f}{2n_s} \tag{25}$$

4. EXPERIMENTAL RESULTS AND DISCUSSION

Since the bubble size is a series of discrete random variables, we must describe the PDF of bubble size before using B-spline estimation. In statistics, kernel density estimation is a non-parametric way to estimate the probability density function of a random variable and it has been applied in many fields such as signal processing, econometrics and so on. In this paper, we use kernel density estimator with the kernel of "triangle" to estimate the PDF of bubble size distribution, and then the B-spline estimation is adopted to approximate the kernel density estimate.

Fig. 5 shows the kernel density estimate of bubble size and the approximation by B-splines according to Fig. 4.

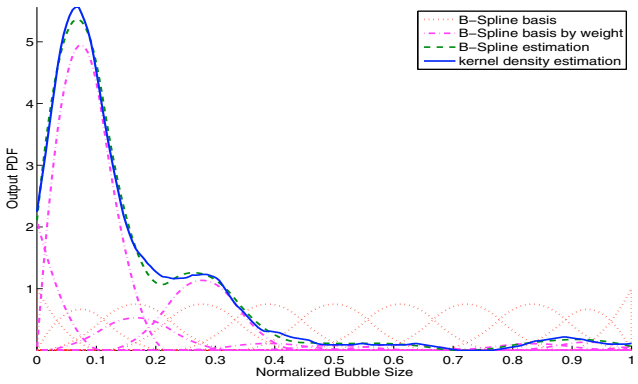

Fig. 5. PDF estimation by B-spline and kernel

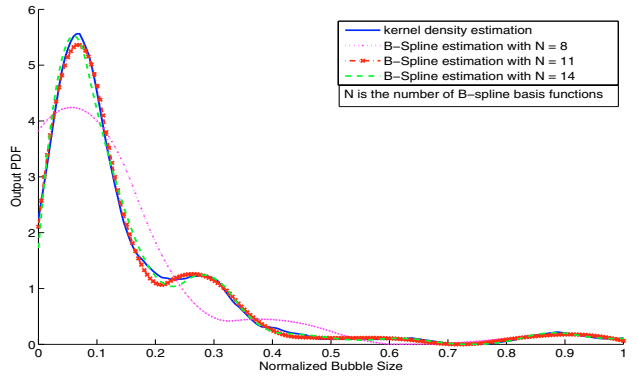

Fig. 6. PDF estimation by B-spline with different numbers of basis function

Red dotted lines represent the basis function of B-spline. Purple dotted lines mean the weighted basis function. B-spline estimation denoted by green dotted line is the combination of weighted basis functions. Blue line means the kernel density estimate. As shown in Fig. 5, B-spline estimation can approximate the kernel density estimate accurately. However, since the B-spline basis functions are fixed, the B-spline estimation is only determined by weight vector. It means that the control of bubble size distribution can convert to the control of B-spline weight vector. This experiments proved the feasibility of using B-spline function to estimate the bubble size distribution.

Table 1. Calculated results of B-spline estimation with different numbers

n	least square error	entropy
7	52.2358	-0.6946
8	40.6680	-0.6319
9	22.8605	-0.6446
10	7.4507	-0.6858
11	1.0002	-0.7266(min)
12	0.9956	-0.7216
13	1.9203	-0.7113
14	2.1437	-0.7062
20	0.2707	-0.6628
21	0.1623	-0.6553

Table 1 and Fig. 6 are the experiment results of B-spline estimation with different number of basis functions. In table 1, when n increases from 7 to 21, the least square error of B-spline estimation is also changed. With different n, the basis functions of B-spline are different. So the least square error can not decrease with the decrease of n. The entropy is used to evaluate the model of B-spline estimations, and it dose not have decreasing property with number of basis functions of B-spline. After calculating the entropy, B-spline estimation with $n = 11$ is chosen as the best model.

In Fig. 6, blue line is the kernel density estimate of bubble size which can be considered as a target distribution, green, red and purple dotted line represent the B-spline estimation with $n = 14$, $n = 11$, $n = 8$ respectively. It is clearly revealed that purple dotted line is worse than others. Both green dotted line and red dotted line can fit the given PDF, but the green dotted line is distorted when describe the peak and valley points of the curve. Red dotted line can match the given PDF in most cases and the bubble size with maximum probability is similar to the given data.

5. CONCLUSION

As one of the important visual features, bubble size distribution has great effect on dealing with the control problem of froth flotation. In order to analyze the distribution of bubble size quantitatively, the entropy-based estimation is used in this paper. First, the PDF of bubble size distribution is described by using kernel density estimators. Second, the least square method is applied to approximate the kernel density estimate with B-spline estimation, and then the entropy analysis is adopted to choose the best model of B-spline. The estimation results of B-spline function and kernel function have proved that the B-spline estimation is able to fit PDF effectively. Besides, experiments about the determination of the best B-spline model have shown that the evaluation mechanism based on the entropy analysis can identify the number of B-spline basis functions, which have testified the feasibility of the proposed method. In the future, we will study multi-frame images to handle uncertainties and disturbances in the PDF of bubble size.

REFERENCES

Bao, L., Bodil, R., Jørgen, K., Sten, B., (2008). Bubble size estimation for flotation processes. *Minerals Engineering*, volume 21, 539–548.

Bartolacci, G., Serranti, S., Volpe, F., Zuco, R., (2001) Characterization of flotation froth structure and color by machine vision. *Comput. Geosci.*, volume 27, 1111–1117.

Feng, D., Aldrich, C., (2000). The effect of frothers on bubble size distributions in flotation pulp phases and surface froths. *Minerals Engineering*, volume 13(10), 1049–1057.

Forbes, G., (2007). Texture and bubble size measurements for modeling concentrate grade in flotation froth systems. *Struct. Saf.*, volume 20, 106–119.

Guo, L., Wang, H., Wang, A., (2008). Optimal probability density function control for NARMAX stochastic systems. *Automatica*, volume 44(7), 1904–1911.

Liu, J., Macgregor, J., Duchesene, C., Bartolacci, G., (2005). Flotation froth monitoring using multiresolutional multivariate image analysis. *Miner. Eng*, volume 18, 65–76.

Mood, A., Graybill, R., Boes, D., (1974). Introduction to the theory of statistics. *International Student Edition*. 3rd edition.

Moolman, D., Eksteen, J., Aldrich, C., Vandeventer, J. (1996). The significance of flotation froth appearance for machine vision control. *International Journal of Mineral Processing*, volume 48(3/4), 135–158.

Wang, W., Bergholm, F., Yang, B., (2003). Froth delineation based on image classification. *Miner. Eng*, volume 16, 1183–1192.

Wang, W., Li, L., (2005). Image analysis and computer vision for mineral froth C. *Proc. IEEE Int. Conf. Mechatron. Autom.*, volume 4, 1790–1795.

Wang, Y., Neethling, S., (2009). The relationship between the surface and internal structure of dry foam. *Colloids and Surfaces A: Physicochemical and Engineering Aspects*, volume 339(1–3), 73–81.

Wu, J., Xie, Y., Gui, W., Yang, C., (2015). Mineral concentration estimation of feed ore in gold and stibium flotation based on froth image features. *Control Theory and Applications*, volume 32(2), 262–266.

Yang, C., Xu, C., Mu, X., Zhou, K., (2009). Bubble size estimation using interfacial morphological information for mineral flotation process monitoring. *Transactions of Nonferrous Metals Society of China*, volume 19, 694–699.

Yang, C., Xu, C., Gui, W., Du, J., (2009). Nonparametric density estimation of bubble size distribution for monitoring mineral flotation process. *In: 48th IEEE Conference on Decision and Control*. Shanghai, 2941–2945.

Zhang, Y., Guo, L., Wang, H., (2006). Filter-based fault detection and diagnosis using output PDFs for stochastic systems with time delays. *Control Signal Process*, volume 20(1), 175–194.

Zhu, J., Gui, W., Yang, C., Xu, H., Wang, X., (2014). Probability density function of bubble size based reagent dosage predictive control for copper roughing flotation. *Control Engineering Practice*, volume 29, 1–12.

Zong, Z., Lam, K., (1998). Estimation of complicated distributions using B-spline functions. *Control Signal Process*, volume 20(4), 341–355.